R.H. Middleton, T. Wigren, K. Lau, and R.A. Delgado. **Data Flow Delay Equalization for Feedback Control Applications Using 5G Wireless Dual Connectivity**. In *IEEE 85th Vehicular Technology Conference (VTC2017-Spring)*, Sydney, Australia, 2017.

Available at https://doi.org/10.1109/VTCSpring.2017.8108608

Data Flow Delay Equalization for Feedback Control Applications Using 5G Wireless Dual Connectivity

Richard H. Middleton
Priority Research Centre for
Complex Dynamic Systems and Control
The University of Newcastle
Callaghan, NSW 2308, AUSTRALIA
richard.middleton@newcastle.edu.au

Torbjörn Wigren
L5GR Systems
Ericsson AB
SE-16480, Stockholm
SWEDEN
torbjorn.wigren@ericsson.com

Katrina Lau and Ramón A. Delgado
Priority Research Centre for
Complex Dynamic Systems and Control
The University of Newcastle
Callaghan, NSW 2308,AUSTRALIA
{k.lau,ramon.delgado}@newcastle.edu.au

***Abstract*—The emerging 5G networks are intended to enable new feedback control applications, run over multiple wireless interfaces. 5G wireless technologies then need to match the state-of-the-art wired network performance, experienced by present commercial feedback control systems. Fibre-optic circuit switched communication is characterized by constant and very low loop delays, uniform and very high sampling rates, very low error rates and an almost unlimited capacity. The non-trivial challenge is then to meet these characteristics with a packet switched wireless 5G network that may be associated with varying latency, time varying sampling rates, significant error rates and a varying air-interface capacity. The paper contributes with a summary and discussion of basic requirements that need to be in place for successful commercial deployment of feedback controllers using such 5G wireless networks. One key requirement is a need to mitigate the problem of delay skew between different transmission paths. A novel delay skew data flow control algorithm is therefore proposed for 5G dual connectivity. The stability of the controller is analyzed and conditions for global $\mathcal{L}_2$-stability are stated. Test bed results are also reported in the paper, indicating that the delay skew controller can meet the requirements on the delay characteristics of 5G networks.**

I. Introduction

Fifth generation wireless networks aim to expand wireless technology to new fields of application, among these feedback control using critical machine-type communications (C-MTC) [4]. Examples of new use cases include massive high bandwidth industrial mobile robot control [20] and the tactile internet [9], [10], where virtual reality is expected to become a significant use case [14]. Automatic control of rotating machinery also benefits, since wireless feedback signaling avoids the need for electro-mechanical devices like slip rings [1].

However, the reduced latency of the new 5G wireless interfaces is only one of several enablers for a successful deployment of feedback control applications. The reason is that the 5G networks will be packet switched, sometimes with control algorithms located in the cloud, resulting in feedback control application data transfer over shared internet connections. This means that the end to end data transport performance experienced by the feedback control applications may be subject to varying delay, non-uniform sampling, data errors, and a varying capacity caused by wireless fading [11], [13]. These effects are obviously less pronounced when dedicated fibre-optic and copper wire based communication is used. Therefore, to enable the cost saving and increased flexibility associated with a replacement of wire, 5G wireless networks may need to be further controlled to reduce the challenges listed above. An additional challenge arises when millimeter-wave carrier frequencies are used, since the increased radio shadowing then makes multi-point wireless transmission needed for coverage reasons [4], [11]. The feedback control application data signaling may then also need to be split over multiple paths, while keeping the delay characteristics aligned between the different transmission paths. New methods for delay control are therefore needed in support of 5G wireless networked feedback control applications. This fact has also been noticed by the IEEE control systems society in [12].

The contributions of the paper therefore include a first discussion of the effect of delay, delay variation, sampling and capacity, on feedback controllers and control systems running over packet switched 5G multi-point transmission networks. This motivates the need for network control algorithms that mitigate the challenges caused by the packet switched wireless combination. As a second contribution, a non-linear round trip delay skew feedback controller for 5G dual connectivity (DC) based C-MTC is proposed. This controller ensures that the packet switched data transport used by the C-MTC application feedback controllers is characterized by better defined delay properties. The round trip delay skew algorithm is also proved to be globally stable. It is stressed that this is a practically relevant result, since the C-MTC applications rely on stable delay properties of the underlying data transport, *at all times*. The control algorithm is also evaluated using a test bed C++ implementation. The obtained results show that the algorithm can regulate away the delay variations discussed above.

Recent work related to the present paper include [2], [3], [8] and [19]. The paper [2] also treats a delay skew controller for C-MTC. The present paper differs in that the focus is on general (delay) requirements for C-MTC. In addition, the non-linear processing differs, thereby allowing a stability analysis based on a combination of the Nyquist- and Popov-criteria [15], rather than on the more advanced integral quadratic constraint (IQC) method [7] used for the $n+1$-node controller

treated in [2]. The DC algorithm described in [19] is designed to control the delay skew from the data split point to the downlink wireless interface, thereby securing the simultaneous reception of originally adjacent data packets, in the mobile. The control objective of the present paper is different and focused on control of the round trip delay skew from the data packet split point to the mobile interface connecting to the controlled plant at the other side of the air interface, and back. This provides the possibility to control the loop delays experienced by feedback control applications. One consequence as compared to [19], is that the inner control loops need to be selected as the one described in [17]. The papers [3] and [8] both treat a multi-point delay skew controller for control of the downlink delay skew, as in [19]. Here [8] treats classical sensitivity and regulation performance properties, while [3] analyzes the stability properties with IQC methodology.

The layout of the paper is as follows. Section II is focused on requirements for feedback control over wireless connections. The round trip delay skew control algorithm is then outlined in section III and evaluated in section IV. The paper ends with concluding remarks in Section V.

II. C-MTC REQUIREMENTS FOR FEEDBACK CONTROL APPLICATIONS

Control systems are best designed from empirical and/or theoretical models. Very often, linear models are used, see e.g. [5]. In practice, various constraints also need to be accounted for and in such cases linear models may be augmented with constraint handling using model predictive control [6]. As will be seen, the possibility to easily apply the standard controller design techniques depends on well defined delay properties of the bearer of the control system signals. Later in the paper the exact location of the controller node, the network delays, the wireless interfaces and the plant node with the UE interface will be defined. In the present section, the effect of delay is considered from the point of view of the feedback control application. In particular, wireless packet switched delay effects are characterized. This leads to the formulation of a set of basic requirements for 5G network design.

A. Effects of delay on stability

To quantify the effect of delay on stability it is assumed that the continuous time transfer function of the linear system is given by $G(s)$ and that the transfer function of the controller is given by $C(s)$, where s is the Laplace transform variable. In addition the closed loop system is affected by a round trip loop delay T. The loop gain of the system is then given by

$$\hat{g}(s) = C(s)G(s)e^{-sT}. \tag{1}$$

Under mild conditions the stability of the closed loop linear system of Fig. 1 is then given by

Nyquist Criterion, [15] Theorem 6.6.58: The system with loop gain $\hat{g}(s)$ of Fig. 1 is $\mathcal{L}_2$-stable if and only if the Nyquist plot

$$\omega \in [0, \infty) \rightarrow Re[\hat{g}(j\omega)] + jIm[\hat{g}(j\omega)] \in \mathcal{C}$$

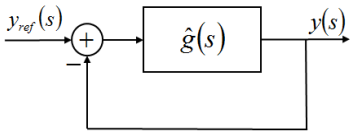

Fig. 1. Simple feedback.

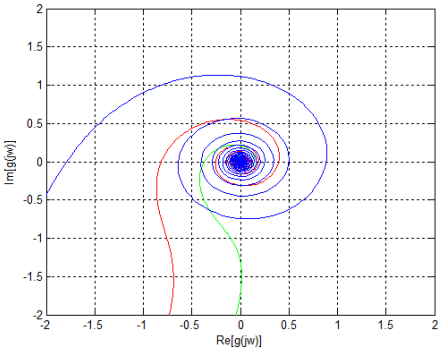

Fig. 2. Nyquist plots for delays of $T = 0.005$ s (green), $T = 0.015$ s (red) and $T = 0.045$ s. (blue).

is bounded away from and does not encircle $-1 + j0$.

Here ω denotes the angular frequency. $\mathcal{L}_2$-stability implies that all internal signals $x(\cdot)$ of the closed loop system are finite in the sense that

$$\int_0^\infty |x(t)|^2 dt < \infty, \tag{2}$$

provided that the external inputs meet the same condition [15].

As an illustration, Nyquist plots for varying delays are shown for the lead lag controller structure of [19]. The illustrated control system has a loop gain given by

$$\hat{g}(s) = 69.43 \frac{(s + 2.30)}{(s + 0.23)} \frac{(s + 30.49)}{(s + 69.51)} \frac{1}{s} e^{-sT}. \tag{3}$$

It can be seen that the loop is stable for delays up to just above 15 ms. It is evident that the delay of the loop needs to be kept low enough to secure stability.

B. Effects of delay on regulation performance

As may also be seen in Fig. 2, an increasing delay causes the critical point of intersection between the Nyquist plot and the negative real axis to correspond to a point further out on the Nyquist plot. The shape of the Nyquist plot is also changed. This is analyzed in [16]. To understand the main result of [16] the sensitivity function $S(s)$ needs to be defined [5]. Fig. 3, where $w(s)$ denotes a disturbance, gives

$$y(s) = (1 - S(s))y_{ref}(s) + S(s)w(s), \tag{4}$$

where

$$S(s) = \frac{1}{1 + C(s)G(s)e^{-sT}} = \frac{1}{1 + \hat{g}(s)}. \tag{5}$$

The sensitivity function is central in control and quantifies the suppression of an unwanted disturbance $w(s)$ on the output

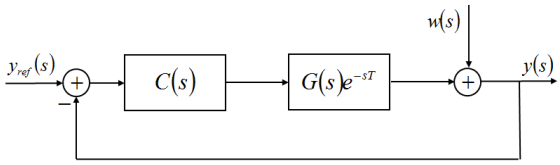

Fig. 3. Block diagram defining the sensitivity function $S(s)$.

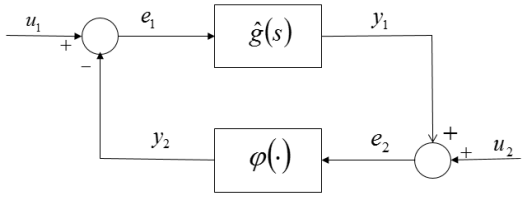

Fig. 4. Block diagram for which the Popov criterion is formulated. u_1 and u_2 are external input signals.

signal. To obtain good suppression the loop gain needs to be high. As shown next this is not possible when the delay increases. In order to study the effect of large delays on the sensitivity function a system with an additional saturation in the control loop is considered, as shown by Fig. 4. The saturation is given by

$$\varphi(u) = \begin{cases} ku_{max}, & u \geq u_{max} \\ ku, & u_{min} < u < u_{max} \\ ku_{min}, & u \leq u_{min} \end{cases} . \quad (6)$$

Here k is the static gain, while u_{min} and u_{max} denote the saturation limits. The reason for the inclusion of a saturation is that control signal limitations are of central importance e.g. in servo control applications [5], [15]. The analysis therefore becomes nonlinear, and it is based on the Popov criterion given by

Popov Criterion, [15] Theorem 6.7.63: Consider the system of Fig. 4. Assume that the time invariant static nonlinearity $\varphi(\cdot)$ fulfils

$$0 \leq \sigma\varphi(\sigma) \leq k\sigma^2,$$

and that $u_1 \in \mathcal{L}_2$, $u_2 \in \mathcal{L}_2$, $\dot{u_2} \in \mathcal{L}_2$. Under these conditions the system is $\mathcal{L}_2$-stable if there exist constants q, δ, such that the Popov plot

$$\omega \in [0, \infty) \rightarrow Re[\hat{g}(j\omega)] + j\omega Im[\hat{g}(j\omega)] \in \mathcal{C}$$

is entirely to the right of a line through $-1/k + \delta + j0$ with slope $1/q$, for some $q \geq 0$ and some $\delta > 0$.

In the analysis of [16], the case where $T \rightarrow \infty$ is considered. The key step is to use the Popov criterion and to prove that the limiting case when $T \rightarrow \infty$ can instead be analyzed by the case where $\omega \rightarrow 0$. This means that the interpretation given by the first sentence of this subsection is indeed true. When the Popov criterion is applied for $\omega \rightarrow 0$, it follows that $\mathcal{L}_2$-stability cannot hold if

$$\hat{g}(0) > \frac{1}{k}. \quad (7)$$

Equations (4) and (5) then imply

Theorem 3, [16]: Consider a control loop with a strictly proper asymptotically stable linear dynamic loop gain, together with a delay T and a saturation. Then, when $T \rightarrow \infty$, The Popov criterion cannot imply $\mathcal{L}_2$ stability whenever

$$S(0) \leq \frac{k}{k+1}.$$

The consequence is that when the delay becomes large, steady state disturbances cannot be suppressed below a certain level, without risking stability of the control loop.

C. Effects of delay variation on feedback control

Packet switched networks are subject to delay variation. The present sub-section illustrates the effects such a variation may have on the application controllers that use the bearers of the packet switched network.

1) Sampling, computational complexity, controller design and stability: To begin, consider the system $G(s)$ of (1), and assume that sampled feedback signals are available at the set of times $\{t_k\}$, $k = 0, 1, ...$ To transfer the system to discrete time form, $G(s)$ is first written in state space form as the following ordinary differential equation (ODE)

$$\dot{x}(t) = Ax(t) + Bu(t) \quad (8)$$

$$y(t) = Cx(t). \quad (9)$$

Here $x(t)$ is the state vector, A the system matrix, B the input gain matrix, $u(t)$ the control signal, $y(t)$ the output signal and C the output matrix. The sampling of the ODE is performed by solving (8) assuming a constant input signal between the sampling instances, i.e. a zero-order-hold (ZoH) sampling. Following [5], chapter 4, and solving from t_k to t_{k+1} gives

$$\begin{aligned} x(t_{k+1}) &= e^{A(t_{k+1}-t_k)}x(t_k) + \int_{t_k}^{t_{k+1}} e^{A(t_{k+1}-\tau)}Bu(\tau)d\tau \\ &= F(t_{k+1}, t_k)x(t_k) + G(t_{k+1}, t_k)u(t_k). \end{aligned} \quad (10)$$

Here $F(t_{k+1}, t_k)$ is the discrete time system matrix and $G(t_{k+1}, t_k)$ is the discrete time input gain matrix. The static output equation (9) is transformed into

$$y(t_k) = Cx(t_k). \quad (11)$$

When the sampling is uniform, i.e.

$$\{t_k\} = \{kT_s\}, \ k = 0, 1, ... \quad (12)$$

where T_s is the sampling period, the discrete time system and input gain matrices simplify to

$$F(t_{k+1}, t_k) = F = e^{AT_s}, \quad (13)$$

$$G(t_{k+1}, t_k) = G = A^{-1}(e^{AT_s} - I)B. \quad (14)$$

It is a significant advantage that (13) and (14) can be pre-computed since that reduces the computational complexity of (10) significantly. In addition to the computational aspects, it is stressed that the stability analysis of a time varying system is more difficult than the one for a time invariant one, see

e.g. [15]. Since stability is such an important engineering property, time variable models are often avoided. Nevertheless, several controller design methods do allow a time varying model, among them the Linear Quadratic Gaussian (LQG) design method [5]. However, since both the system matrices and the controller gains need re-computation at each sampling instance, the computational complexity is much higher than for the time invariant counterpart based on uniform sampling. Another advantage of using uniform sampling together with linear systems is the wide variety of standard controller design methods. I

2) Effects of varying data flow delay: When the delay of the packet switched data bearer is varying, the delay between transmission of controller commands $u(t_k)$ from a controlling node to the arrival of feedback information from the plant at the other side of the air interface also varies. The consequence is that uniform sampling instances at the controller node become asynchronous with the feedback signals.

One solution is then to *define* the sampling instant as the time when feedback information arrives back at the controlling node. This allows a use of the exact sampling relation (10). The penalty would be a very significant computational cost.

A second solution would be to enforce uniform sampling and to take action to account for the resulting sampling errors. To compute these errors, it is assumed that t_k^* is the latest instance when a sample is taken preceding kT_s, and that t_{k+1}^* is the next instance when a sample is taken. The sampling instances are defined by the arrival of feedback information in the controller node. It is also assumed that $u(t_k^*)$ is used in the interval $kT_s \leq t < (k+1)T_s$, that $x(kT_s)$ is approximated with $x(t_k^*)$, and that equations (13) and (14) are used, to enforce uniform sampling. This means that the state error, at the sampling instances, obey

$$\Delta x(kT_s) = e^{A(kT_s - t_k^*)} x(t_k^*)$$
$$+A^{-1}(e^{A(kT_s - t_k^*)} - I)Bu(t_{k-1}^*) - x(t_k^*),\ t = kT_s, \quad (15)$$

$$\Delta x((k+1)T_s) = F(x(t_k^*) + \Delta x(kT_s)) + Gu(t_k^*)$$
$$-Fx(t_k^*) - Gu(t_k^*) = F\Delta x(kT_s),\ t = (k+1)T_s. \quad (16)$$

It can be seen that $\Delta x(kT_s)$ is small whenever the error of the sampling instances is small. The error of (16) manifests itself as a modeling error. The controller design then requires a corresponding back-off to maintain stability. This results in a degradation of performance, c.f. [5] chapter 6.

D. C-MTC capacity dimensioning

To estimate the air interface capacity needed to sustain closed loop feedback control of high bandwidth robotic machinery in a manufacturing plant using wireless connections, a rough dimensioning example is useful.

Example 1: Consider a plant with 100 mobile robots used for manufacturing purposes. Assume that there are 10 degrees of freedom of each robot, requiring one feedback signal and one control signal each. Assuming a required bandwidth of 250 Hz leads to a sampling frequency close to 5 kHz (10 times the Nyquist frequency), a figure consistent with current 5G standardization. A round trip loop delay of 1 ms or better is needed to avoid a too large phase loss. If all signals are encoded with 4 bytes, and if a code rate of 1/5 is assumed, the total bit rate for each machine becomes $2 \times 10 \times 4 \times 8 \times 5000 \times 5\ bits/s = 16\ Mbit/s$. The plant therefore requires a capacity exceeding 1.5 $Gbit/s$. This is reasonable for the first 5G DC deployments. In case 0.5 ms is allocated for transmit data buffering, user data corresponding to 1000 bytes per machine will reside in each buffer on average.

E. Requirements

It should now be clear that in case a packet switched bearer of control information is associated with a large delay, feedback control stability margins, disturbance rejection performance and closed loop bandwidth are negatively affected. In addition, in case of significant delay variations, additional negative impacts is likely to affect the application performance. The feedback control system application may either need to resort to time varying controller design, a path that can result in a very high computational complexity, or it has to apply additional margins to account for sampling errors. Such margins tend to reduce the performance of the application. Finally, the high capacity that may be needed then dictates that air interface resources need to be efficiently used. In particular this means that data should (almost) always be available at the air-interface for transmission

Together this means that the following basic requirements can be stated for the use of 5G packet switched wireless networks for automatic control.

- *Loop delay*: The round trip (single path) loop delay should be minimized.
- *Utilization*: The air interfaces should (almost) always be fully utilized.
- *Delay variation*: The round trip delay variation should be minimized.
- *Delay alignment*:Round trip delays over multiple air interfaces should be aligned.

In the following section a new delay skew control algorithm is introduced. This algorithm is designed to control the loop delays, while simultaneously managing the utilization and aligning the loop delays.

III. Round trip delay skew control for 5G dual connectivity

A. Dual connectivity for C-MTC in 5G

5G DC allows simultaneous transmission over two wireless interfaces. This improves reliability when radio shadowing occurs at high carrier frequencies [11]. Fig. 5 shows that the plant controllers are assumed to be located in or near the primary/controller node to minimize latency. Control signals and feedback signals are sent between the plant controllers and the plant at the other side of the wireless interfaces. To meet the delay alignment requirement an outer loop round trip delay skew controller is operating in the primary node, below the application layer, c.f. [19]. The transmit data queues buffer

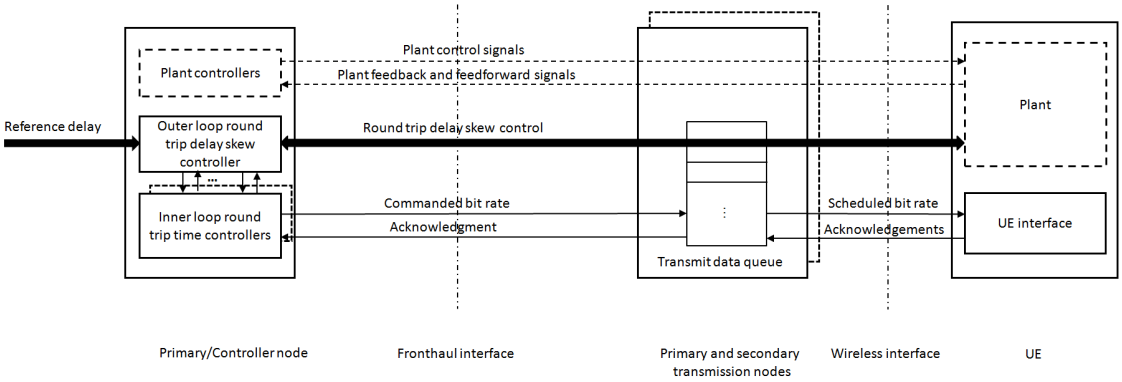

Fig. 5. C-MTC layers in 5G dual connectivity. In case networked adaptive controllers would be run at the application layer, recursive networked identification algorithms would be needed as well, c.f. e.g. [18] and [21]

against fast fading, securing that the air interfaces experience a high utilization. They are also the actuator compensating for the possibly varying fronthaul delays. The inner loops control the data packets in flight so that the round trip delays computed by the outer loop controller are met. Further details on DC is available in [17] and [19].

B. Round trip delay skew cascade control

The round trip delay skew controller is depicted in Fig. 6. As can be seen there are two inner loops, one handling the data transfer for the primary node and one handling the data transfer for the secondary node. These inner loop controllers are window based [17]. They control the time of flight for application data packets from the data split point, over the fronthaul interface to one of the transmission nodes, to the user equipment (UE) interface of the plant node, and back until the acknowledgment corresponding to each package is received back at the data split point. The flow is strictly one directional which means that there is a saturation in each inner loop controller. The inner loop controllers utilize high gain static feedback. The reason is that this results in global $\mathcal{L}_2$-stability, irrespective of the static feedback gain and the round trip loop delay [17]. As motivated in detail in [2] and [17], the inner loop controllers can be modeled by the transfer functions

$$G_i^{inner}(s) = \frac{C_i\left(1-e^{-sT_i^{RTT}}\right)}{s+C_i\left(1-e^{-sT_i^{RTT}}\right)},\ i=1,2. \tag{17}$$

Here T_i^{RTT}, $i=1,2$, denotes the round trip delay of each inner loop, while C_i, $i=1,2$ denotes the static feedback gain of each inner loop. Note that (17) assumes that the saturations of the inner loops represent inactive constraints, with the linear region of the saturations having unity gains. The first condition can be enforced with a proper reference value setting, adding delay to the total delay budget that is set by $T_{ref,sum}^{RTT}(s)$.

The outer round trip delay skew control loop of Fig. 6 operates as follows. The round trip delays $T_1^{RTT}(s)$ and $T_2^{RTT}(s)$ are obtained from each inner loop. The delay sum control channel acts as the reference channel, while the delay skew is handled by the delay skew control channel. Therefore the following feedback signals are formed

$$T_{skew}^{RTT}(s) = T_1^{RTT}(s) - T_2^{RTT}(s), \tag{18}$$

$$T_{sum}^{RTT}(s) = T_1^{RTT}(s) + T_2^{RTT}(s). \tag{19}$$

The error signals are then formed for each channel, where

$$e_{skew}^{RTT}(s) = T_{ref,skew}^{RTT}(s) - T_{skew}^{RTT}(s), \tag{20}$$

$$e_{sum}^{RTT}(s) = x_2(s) = T_{ref,sum}^{RTT}(s) - T_{sum}^{RTT}(s). \tag{21}$$

Here $T_{ref,skew}^{RTT}(s)$ and $T_{ref,sum}^{RTT}(s)$ are the reference signals. Typically $T_{ref,skew}^{RTT}(s) = 0\ s$, while $T_{ref,sum}^{RTT}(s)$ is set to a value consistent with the total round trip time delay budget for the round trip delay skew controller. For a $1\ ms$ requirement the total delay budget would e.g. be $2\ ms$. The skew control error is also processed by the following time domain deadzone

$$x_1(t) = \begin{cases} e_{skew}^{RTT}(t) - \Delta T_{skew}, & e_{skew}^{RTT}(t) > \Delta T_{skew} \\ 0.0, & |e_{skew}^{RTT}(t)| \leq \Delta T_{skew} \\ e_{skew}^{RTT}(t) + \Delta T_{skew}, & e_{skew}^{RTT}(t) < -\Delta T_{skew}. \end{cases} \tag{22}$$

The size of the deadzone is hence given by $\Delta T_{skew} \geq 0$. The deadzone provides a safety net in case the round trip delays would become inconsistent with $T_{ref,sum}^{RTT}(s)$, see [19] for further details. The error signals are then further processed by the outer loop controller filters $C_{skew}(s)$ and $C_{sum}(s)$, followed by a static decoupling to give the reference signals to the inner loops as

$$T_{ref,1}^{RTT}(s) = \frac{1}{2}\left(C_{skew}(s)x_1(s) + C_{sum}(s)x_2(s)\right), \tag{23}$$

$$T_{ref,2}^{RTT}(s) = \frac{1}{2}\left(-C_{skew}(s)x_1(s) + C_{sum}(s)x_2(s)\right). \tag{24}$$

C. $\mathcal{L}_2$ - stability

In [19] a related delay skew controller, with the same structure as in Fig. 6 is proved to be $\mathcal{L}_2$-stable, as stated in Theorem 1 of that paper. The differences to the present paper are that the inner loops are different and that some external signals appearing in the controller of [19] do not appear here. The conditions on the inner loops of [19] state that they shall

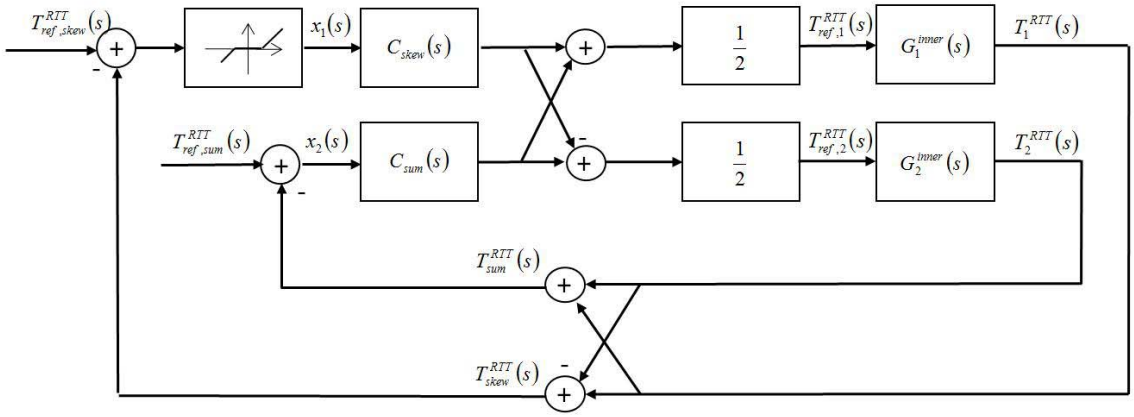

Fig. 6. The round trip delay skew control loop in 5G dual connectivity.

be strictly proper and $\mathcal{L}_2$-stable. As is evident from (17) the inner loops of the present paper have a pole excess of 1 and are hence strictly proper. Furthermore, as proved in [17], the inner loops are always globally $\mathcal{L}_2$-stable. In order to formulate the stability result for the controller of Fig. 6, the following quantities need to be defined.

$$A_{11}(s) = \frac{1}{2}C_{skew}(s)\left(G_1^{inner}(s) + G_2^{inner}(s)\right), \quad (25)$$

$$A_{12}(s) = \frac{1}{2}C_{sum}(s)\left(G_1^{inner}(s) - G_2^{inner}(s)\right), \quad (26)$$

$$A_{21}(s) = \frac{1}{2}C_{skew}(s)\left(G_1^{inner}(s) - G_2^{inner}(s)\right), \quad (27)$$

$$A_{22}(s) = \frac{1}{2}C_{sum}(s)\left(G_1^{inner}(s) + G_2^{inner}(s)\right). \quad (28)$$

The loop gain of the round trip delay skew control channel is also needed. As shown in [19] it is given by

$$\hat{g}(s) = A_{11}(s) - \frac{A_{12}(s)A_{21}(s)}{1 + A_{22}(s)}. \quad (29)$$

The following result now holds

Theorem 1: Consider the round trip delay skew controller of Fig. 6 and assume that A1, A2, A4, A7, A8 and A10 of [19] hold. Then, if the deadzone fulfils

$$0 \leq \sigma\varphi(\sigma) \leq 1\sigma^2$$

and if the Nyquist plot of $A_{22}(s)$ given by

$$\omega \in [0, \infty) \rightarrow Re[A_{22}(j\omega)] + jIm[A_{22}(j\omega)] \in \mathcal{C}$$

is bounded away from and does not encircle $-1+j0$, then the delay skew control system is $\mathcal{L}_2$-stable if there exists constants q, δ, such that the Popov plot of the delay skew control loop gain given by

$$\omega \in [0, \infty) \rightarrow Re[\hat{g}(j\omega)] + j\omega Im[\hat{g}(j\omega)] \in \mathcal{C}$$

is entirely to the right of a line through $-1+\delta+j0$ with slope $1/q$, for some $q \geq 0$ and some $\delta > 0$.

Proof: The proof follows by extraction of the relevant subsets of the proof of Theorem 1 of [19].

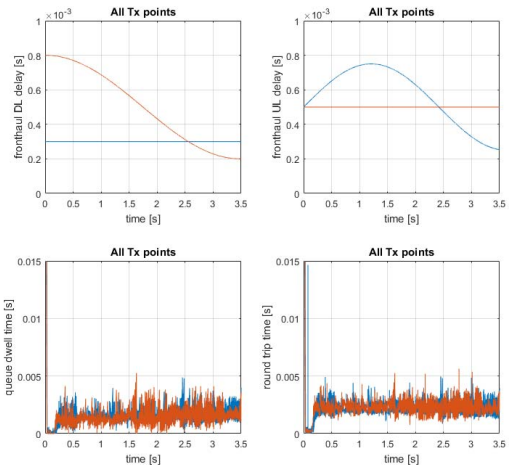

Fig. 7. Fronthaul delays for TX node $i = 1$ red and TX node $i = 2$ blue, together with resulting inner loop queue dwell and round trip times.

IV. Test bed results

The C++ testbed implementation described in [19] was used for performance evaluation. Typical urban channels generated the scheduled wireless rates, driving the delay skew control system. The sampling period was $T_s = 250\ \mu s$. The inner loops used $C = T_s^{-1}$. The reference signals were $T^{RTT}_{ref,skew} = 0.0\ ms$ and $T^{RTT}_{ref,sum} = 5.0\ ms$ meaning that each path was designed for a round trip delay of $2.5\ ms$, good enough e.g. for haptic feedback control. The design procedure described in [2], [19] resulted in the lag filters

$$C_{skew}(s) = C_{sum} = 1.064\frac{s + 69.1}{s + 6.9}. \quad (30)$$

Tustin's approximation was used for discretization of (30) and the deadzone was selected as $\Delta T_{skew} = 0.5\ ms$. Finally, the fronthaul delays varied as shown in Fig. 7 The results of Fig. 8 show that the delay skew controller performs as intended. Note also that the variation of the control signals is consistent with the variation of the front haul delays.

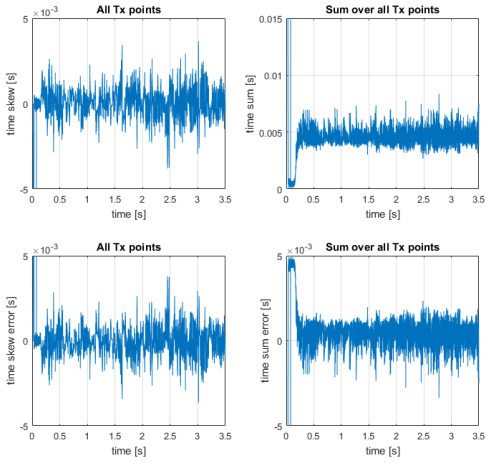

Fig. 8. Delay skew, delay sum and corresponding errors.

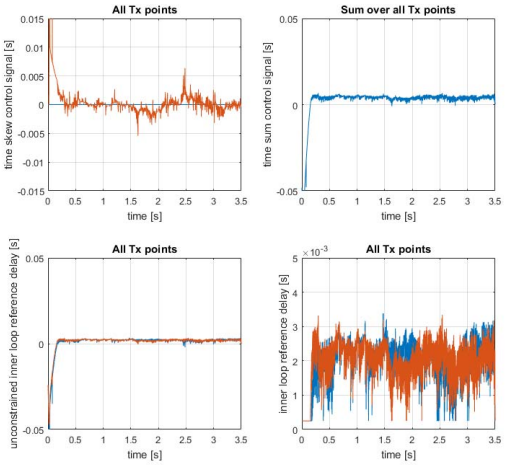

Fig. 9. Control signals.

V. Conclusion

The paper discussed the importance of delay characteristics, when the new 5G wireless networks are used to carry application data for feedback control systems. The effects of delay and delay variation on the stability, performance and computational complexity were treated, resulting in a set of basic requirements that support a successful deployment. It was also shown how a new delay skew controller can be used to align these delay characteristics, between the different transmission paths of 5G dual connectivity. Conditions ensuring a globally stable operation were defined, and testbed results indicate that the delay skew controller is capable of regulating away delay variations, as intended.

Acknowledgment

This research was supported under Australian Research Council's Linkage Projects funding scheme (project number LP150100757).

References

[1] J.-M. Bockard and L. M. Reindl, "Ceramic and magnetic loop antennas for wireless interrogation of SAW resonators on rotation machinery", *IEEE Int. Workshop on Antenna Technology*, pp. 112-115, 2012.

[2] R. A. Delgado, K. Lau, R. H. Middleton and T. Wigren, "Networked Delay Control for 5G Wireless Machine Type Communications Using Multi-Connectivity", *submitted to IEEE Trans. Contr. Systems Tech.*, December, 2016.

[3] R. A. Delgado, T. Wigren, K. Lau and R. H. Middleton, "Stability properties of a MIMO data flow controller", *submitted to CDC 2017*, Melbourne, VIC, Australia, Dec. 12-15, 2017.

[4] Ericsson AB, "5G Radio Access - Research and Vision", *Ericsson White Paper 284 23-3204 Uen*, June, 2013. Available: http://www.ericsson.com/res/docs/whitepapers/wp-5g.pdf.

[5] T. Glad and L. Ljung, *Control Theory.* Bodmin, UK: Taylor and Francis, 2000.

[6] G. C. Goodwin, M. M. Seron and J. A. DeDona, *Constrained Control and Estimation - An Optimization Approach*. London, UK: Springer-Verlag, 2005.

[7] C.-Y. Kao and A. Rantzer, "Stability analysis of systems with uncertain time-varying delays", *Automatica*, vol. 43, no. 6, pp. 959-979, 2007.

[8] K. Lau, T. Wigren, R. Delgado and R. H. Middleton, "Disturbance rejection properties for a 5G networked data flow delay controller", *submitted to CDC 2017*, Melbourne, VIC, Australia, Dec. 12-15, 2017.

[9] T. Marugame, A. Kamikura, M. Ohnishi and M. Nakagawa, "Evaluation on effect of errors on haptic information in wireless communication systems", *Proc. Intelligent Robots and Systems*, vol. 3, pp. 2950-2955, 2003.

[10] J. Pilz, M. Melhouse, T. Wirth, D. Wieruch, B. Holfeld and T. Haustein, "A tactile internet demonstration: 1 ms ultra low delay for wireless communications towards 5G", *IEEE INFOCOM WKSHPS*, pp. 862-863, 2016.

[11] T. S. Rappaport, R. W. Heath Jr., R. C. Daniels and J. N. Murdock, *Millimeter Wave Wireless Communications*. Westford, Massachusetts: Prentice Hall, 2014.

[12] T. Samad, "Control systems and the internet of things," *IEEE Control Systems Magazine*, vol. 36, no. 1, pp. 13-16, 2016.

[13] R. Srikant and L. Ying, *Communication Networks - An Optimization, Control and Stochastic Networks Perspective*. Padstow Cornwall, UK: Cambridge University Press, 2014.

[14] G. Sziebig, B. Solvang, C. Kiss and P. Korondi, "Vibro-tactile feedback for VR systems", *2nd Conference on Human System Interaction*, pp. 406-410, 2009.

[15] M. Vidyasagar, *Nonlinear Systems Analysis*. Englewood Cliffs, NJ: Prentice-Hall, 1978.

[16] T. Wigren, "Low frequency sensitivity function constraints for nonlinear $\mathcal{L}_2$-stable networked control", *Asian J. Contr.*, vol. 18, no. 4, pp. 1200-1218, 2016. DOI: 10.1002/asjc.1241.

[17] T. Wigren and R. Karaki, "Globally Stable Wireless Data Flow Control", *to appear in IEEE Trans Contr. Network Sys.*, 2017. DOI: 10.1109/TCNS.2016.2619906.

[18] T. Wigren, "Networked and delayed recursive identification of nonlinear systems", *submitted to CDC 2017*, Melbourne, VIC, Australia, Dec. 12-15, 2017.

[19] T. Wigren, K. Lau , R. Delgado and R. H. Middleton, "Time skew packet flow control in 5G wireless systems with dual connectivity", *submitted to IEEE Trans. Vehicular. Tech.*, October, 2016.

[20] A. Willig, "Recent and emerging topics in wireless industrial communications: a selection", *IEEE Trans. Ind. Informatics*, vol. 4, no. 2, pp. 102-124, 2008.

[21] S. Yasini and T. Wigren, "Convergence analysis of a networked recursive identification algorithm with output quantization by simulation of associated ODEs", *submitted to CDC 2017*, Melbourne, VIC, Australia, Dec. 12-15, 2017.